GEOPHYSICAL RESEARCH LETTERS, VOL. 27, NO. 16, PAGES 2481-2484, AUGUST 15, 2000

Fractionation of $^{14}N^{15}N^{16}O$ and $^{15}N^{14}N^{16}O$ During Photolysis at 213 nm

Hui Zhang,[1] Paul O. Wennberg,[1,2] Vincent H. Wu[3] and Geoffrey A. Blake[1]

Abstract. Motivated by *Yung and Miller*'s [*1997*] suggestion that N_2O is isotopically fractionated during UV photolysis in the stratosphere, we have studied the photolysis rates of the $^{14}N^{15}N^{16}O$ and $^{15}N^{14}N^{16}O$ structural isotopomers. In this study, we follow the concentrations of these compounds with FTIR spectroscopy during photolysis at 213 nm. When fitted to a Rayleigh fractionation model, the observations yield single-stage enrichment factors of $\epsilon(^{14}N^{15}N^{16}O\ /\ ^{14}N^{14}N^{16}O) = -73 \pm 5$ per mil and $\epsilon(^{15}N^{14}N^{16}O\ /\ ^{14}N^{14}N^{16}O) = -41 \pm 10$ per mil. As predicted by *Yung and Miller* [*1997*], the photolysis rate of $^{15}N^{14}N^{16}O$ is faster than $^{14}N^{15}N^{16}O$ at this wavelength. The magnitude of the observed fractionation, however, is significantly larger than predicted.

Introduction

Nitrous oxide, N_2O, is an important trace gas in the Earth's atmosphere. It is an efficient greenhouse gas and the major source of the nitrogen oxide radicals that destroy stratospheric ozone [*Houghton et al.*, 1995; *WMO*, 1995]. N_2O is produced primarily by biological nitrification and denitrification processes occurring in soils and the oceans, and lost through UV photolysis and reaction with $O(^1D)$ in the stratosphere. It has been established that the present concentration of N_2O in the atmosphere is 8% higher than the pre-industrial value and that it is increasing at a yearly rate of about 0.25%. N_2O is targeted by the 1997 Kyoto Protocol on Climate Change for regulation. This is a difficult task, however, because the global budget for N_2O is poorly quantified. The strength of the sources identified to date can only account for approximately two-thirds of the sum of the well-established sinks and the accumulation in the atmosphere.

Stable isotope analysis can provide useful constraints on the strength of the sources and sinks for atmospheric species. Numerous studies have been performed to investigate the isotopic fractionation of N_2O in various production and loss processes using the stable isotope analysis [*Wahlen et al.*, 1985; *Yoshinari et al.*, 1985; *Yoshida et al.*, 1988; *Kim et al.*, 1990, 1993; *Yoshinari et al.*, 1997; *Cliff et al.*, 1997; *Rahn et al.*, 1997; *Naqvi et al.*, 1998]. These measurements reveal that, relative to tropospheric N_2O, the major biological sources of N_2O are light in both ^{15}N and ^{18}O, while stratospheric N_2O is found to be isotopically heavy. To utilize these isotopic data to characterize the N_2O global budget, one must understand the fractionation induced by biological processing and photolysis in the atmosphere. In an effort to explain the heavy stratospheric N_2O, *Yung and Miller* [1997] (YM97) proposed a wavelength-dependent enrichment mechanism during UV photolysis. They suggested that the difference in the zero point vibrational energy (ZPE) for the heavier N_2O isotopomers causes a blue-shift in the UV cross sections. This blue-shift, when convolved with the spectral characteristics of the actinic flux, produces fractionation. Experiments using laser photolysis and mass spectrometry have been conducted to test one aspect of this theory [*Rahn et al.*, 1998]. It has been shown that UV photolysis of N_2O at 207 nm and 193 nm results in significant enrichment in both ^{15}N and ^{18}O with larger fractionations at longer wavelengths. This is consistent with YM97 though the observed enrichment factor is more than that predicted by the simple ZPE calculations [*Rahn et al.*, 1998].

Yung and Miller [1997] also pointed out that, since the ZPEs are different for $^{14}N^{15}N^{16}O$ and $^{15}N^{14}N^{16}O$, there should also be a differential fractionation between these two structural isotopomers during UV photolysis. In this paper, we use Fourier Transform Infrared (FTIR) spectroscopy in conjunction with laser photolysis to study the fractionation between $^{14}N^{15}N^{16}O$ and $^{15}N^{14}N^{16}O$ at 213 nm.

Experimental

Figure 1 presents a schematic of our experimental set up. UV photons are generated by a Nd:YAG laser, while IR spectra are collected with an FTIR spectrometer. The general experimental procedure is to photolyze the N_2O sample continuously while taking IR spectra to monitor the concentration of the isotopomers.

The photolysis is conducted at 212.8 nm (abbreviated as 213 nm hereafter). This wavelength is chosen primarily because it is conveniently produced by the 5th harmonic generation of a Nd:YAG laser. The fundamental output of the YAG laser (Coherent) is first doubled to 532 nm. The 532 nm is then doubled using a 2-mm thick β-BaB_2O_4 (BBO) crystal. In a second thin BBO crystal, 266 nm light is mixed with the residual 1064 nm radiation to generate 213 nm pulses. The two crystals are cut for type I phase matched 4th and 5th harmonic generation of the 1064 nm fundamental. A single quartz Pellin Broca prism is used to separate 213 nm from the other wavelengths, which are intercepted by beam stops.

The photolysis beam enters the FTIR spectrometer (Magna–IR 560 from Nicolet) through a quartz window (W_1) after the 45° turning mirror (M_1). It passes into the sample compartment aperture at a steep angle and is redirected by a 0° mirror (M_2) towards a 45° mirror (M_3). Mirror M_3 and

[1] Division of Geological and Planetary Sciences, California Institute of Technology, Pasadena, California
[2] Environmental Engineering Program, California Institute of Technology, Pasadena, California
[3] St. Catharine's College, Cambridge University, Cambridge, UK

Paper number 1999GL011236.
0094-8276/00/1999GL011236$05.00

another 0° mirror (M_4) together pass the UV beam through the sample cell twice. The exiting beam is intercepted by the M_3 mirror mount. All four mirrors (M_1, M_2, M_3 and M_4) are 213 nm high reflectors from Coherent. The spectrometer is oriented so that reflective losses of the photolysis beam on the windows are minimized. During the experiment, the stability of the UV power is monitored with a photodetector (UDT-555UV) through the reflection off window W_1.

The sample cell is made of thick-wall Pyrex glass. It has an inner diameter of ~4 cm and a length of 15 cm. CaF_2 is chosen as the window material because it is transparent in both the IR and UV. The two windows are glued on to the cell with Torr Seal (Varian) at slightly different wedge angles to minimize etaloning.

Three isotopically labeled N_2O samples are used. A pure N_2O sample with natural isotopic abundance is used for $^{14}N^{14}N^{16}O$ (99%+). Separate samples of $^{14}N^{15}N^{16}O$ (98%+) and $^{15}N^{14}N^{16}O$ (98%+) mixed with N_2 (99.999%) at an N_2:N_2O ratio of 40 are purchased from Cambridge Isotopes. The partial pressures of the different gases in the sample mixtures used for the three photolysis experiments are listed in Table 1. All the experiments are conducted at total pressure of approximately 760 torr and at room temperature.

Photolysis (R_1) of N_2O produces $O(^1D)$, which reacts with N_2O (R_2):

$$N_2O + h\nu \longrightarrow N_2 + O(^1D) \qquad (R_1)$$

$$O(^1D) + N_2O \longrightarrow NO + NO(60\%) \qquad (R_2)$$
$$\longrightarrow N_2 + O_2(40\%).$$

To prevent N_2O from being oxidized (R_2), $O(^1D)$ quenching by N_2 or CO_2 is necessary:

$$O(^1D) \xrightarrow{M} O(^3P). \qquad (R_3)$$

In Exp. II and III, only one rare N_2O isotopomer is involved and N_2 serves as the quenching gas. For an N_2:N_2O ratio of 75, less than 3% of $O(^1D)$ atoms are expected to undergo reaction R_2 due to quenching by N_2 (R_3) [*DeMore et al.*, 1997]. In Exp. I, N_2 quenching is limited by the total cell pressure and the N_2:N_2O ratio of 40 in both the $^{14}N^{15}N^{16}O$ and $^{15}N^{14}N^{16}O$ samples. In this case, CO_2, which is four times more efficient than N_2 at quenching $O(^1D)$, is used as an additional quencher.

The concentration of N_2O is monitored via the Q-branch of the $\nu_2+\nu_3$ combination band, which lies at 2798 cm^{-1} for $^{14}N^{14}N^{16}O$. Shown in Figure 2 are the $\nu_2+\nu_3$ spectra of the three N_2O isotopomers. They are taken at 0.5 cm^{-1} resolution with an MCT/A liquid nitrogen cooled detector. This band is chosen for several reasons. First, it sits in a region free of interference from ambient H_2O and CO_2 absorption (the spectrometer is nitrogen purged). Second, the peaks for the isotopomers are shifted with respect to each other by ~30 cm^{-1} and the small amount of cross interference among them can be easily accounted for. Third, at one atmosphere pressure, the Q-branch is collision-broadened and is fully resolved at 0.5 cm^{-1} resolution. This leads to linear Beer's Law behavior, which is demonstrated in this apparatus by preparing N_2O samples of known concentration using manometry. At 0.5 cm^{-1} resolution, a high SNR can be achieved in approximately 30 minutes (see below for an explanation of the photolysis time scale). For example, in Exp. II, the S/N is more than 100 for the initial spectrum. The signal level is calculated at the center of the Q-branch for $^{14}N^{14}N^{16}O$, while the noise is the root-mean-square (RMS) noise in the baseline between 2850 and 2900 cm^{-1}. Similar SNRs are achieved in the other two experiments.

Table 1. Partial pressures of different gases in the sample mixtures used in the photolysis experiments.

Exp.	$^{14}N^{14}NO$ (torr)	$^{14}N^{15}NO$ (torr)	$^{15}N^{14}NO$ (torr)	Quenching Gas (torr)
I	5	6	5.5	460 (N_2) 280 (CO_2)
II	6	4	-	750 (N_2)
III	6	-	5	750 (N_2)

Approximately 60 mW (2 mJ at 30 Hz pulse repetitive rate) of 213 nm light are used. Over ~11 hours, 70% of the initial N_2O is removed. FTIR scans are co-added, producing one data point every 30 minutes. In addition, spectra are taken before the photolysis to test the spectral processing protocol and data fitting. To monitor any post-photolysis processes, IR spectra are recorded after the photolysis laser is turned off. For the background, spectra of the same pressure of pure N_2 (in Exp. II and III) or the same mixture of N_2 and CO_2 (in Exp. I) are acquired.

The concentration of the isotopomers is derived by first normalizing the co-added spectra against the background. The integrated absorbance of the Q-branch is determined and the retrieved signal is corrected for the small amount of absorption from the other isotopomers.

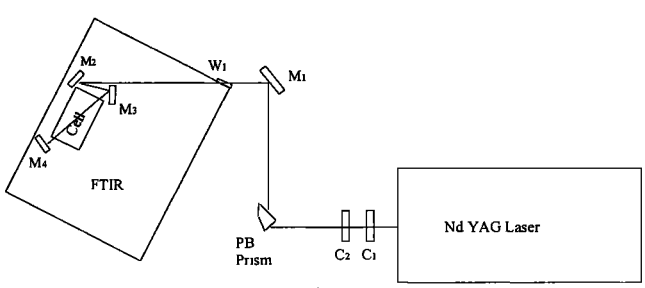

Figure 1. Light from a Nd:YAG laser is directed into the sample compartment of an FTIR spectrometer via a side port. Gas samples are located inside the cell.

Results and Discussion

Figure 3 illustrates the observed fractionation. The slope of the linear fit to the data gives the fractionation factor in a Rayleigh model [*Fritz and Fontes*, 1980]. The results from the three experiments are as follows: $\epsilon(^{14}N^{15}N^{16}O$ / $^{14}N^{14}N^{16}O)$ = -73 ± 5 per mil and $\epsilon(^{15}N^{14}N^{16}O$ / $^{14}N^{14}N^{16}O)$ = -41 ± 10 per mil. The uncertainty results primarily from systematic error introduced in defining the spectral baseline during data processing. The N_2O band is on a sloping region of the IR intensity as shown in Figure 2. A NO_2 band, discussed below, is superimposed nearby on the short-wavelength side of the N_2O $\nu_2+\nu_3$ band. These complicate the spectral analysis. Different techniques for inferring the baseline have been performed and various reasonable assumptions have produced the assigned uncertainty.

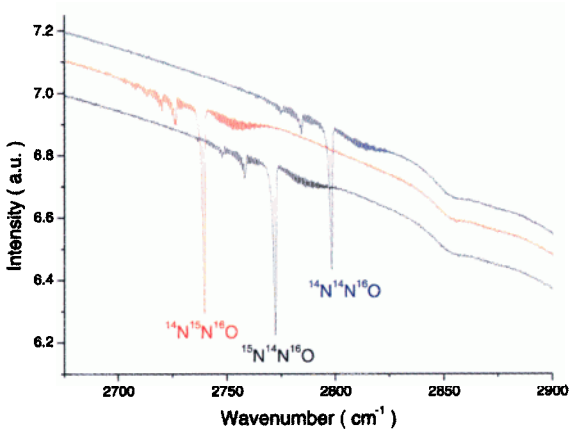

Figure 2.

Figure 2. FTIR spectra of the three N_2O isotopomers, taken between 2650 cm^{-1} and 2900 cm^{-1} at 0.5 cm^{-1} resolution.

The arithmetic average of $\epsilon(^{14}N^{15}N^{16}O$ / $^{14}N^{14}N^{16}O)$ and $\epsilon(^{15}N^{14}N^{16}O$ / $^{14}N^{14}N^{16}O)$ gives -57 ± 15 per mil for $\epsilon(^{15}N$ / $^{14}N)$ at 213 nm. This result is consistent with the results reported by *Rahn et al.* [1998], who observed for $\epsilon(^{15}N$ / $^{14}N)$ values of -18.4 per mil at 193 nm and -48.7 per mil at 207 nm.

We have assumed that all N_2O loss is due to R_1; processes other than R_1 that destroy N_2O would affect our interpretation. One possible interference is R_2, the reaction of $O(^1D)$ with N_2O producing NO. The NO can undergo further conversion to NO_2 in the cell. We have observed the formation of small amounts of NO and NO_2 in each of the three experiments. NO is monitored via its absorption band near 1875 cm^{-1}, NO_2 is monitored at 2907 cm^{-1} and 1617 cm^{-1}. The photolysis of NO_2, whose cross section at 213 nm is more than 1000 times larger than that of N_2O [*DeMore et al.*, 1997], keeps its concentration low while the cell is illuminated with laser light. Once the photolysis ends, however, the NO is converted into NO_2 on the time scale of a few hours. Post-photolysis spectra reveal that the conversion of NO into NO_2 is close to unity. By comparing the photolysis spectra with reference spectra of NO and NO_2, we determine that less than 2% of the N_2O destruction in our experiments have occurred via R_2. This is consistent with the expected quenching rates. Other processes that form N_2O have also been considered. Among them, the three-body reaction of N_2 + $O(^1D)$ to re-form N_2O is extremely slow [*DeMore et al.*, 1997]. Exp. II and III provide a test of whether the photolysis of $^{14}N^{15}N^{16}O$ produces $^{15}N^{14}N^{16}O$ and vice versa. At over 70% photolysis yield, no formation of $^{15}N^{14}N^{16}O$ is observed from the photolysis of $^{14}N^{15}N^{16}O$ and vice versa.

Qualitatively, the observed isotopomer-specific fractionations scale with the ZPE differences noted by YM97. The magnitude of the fractionations found in this experiment (and *Rahn et al.*'s [1998]), however, is significantly larger than predicted by YM97. It appears that the simple ZPE model does not fully account for the observed fractionation. There are a number of reasons why this might be the case. At 298 K, close to 90% of the N_2O is in the ground vibrational state (000) while about 10% is in the first excited bending mode (010). Photodissociation dynamics studies [*Neyer, et al.*, 1999, and refs therein] have shown that the photolysis of N_2O (R_1) occurs mainly via an orbitally forbidden but vibronically allowed transition through a bent excited state. Therefore, the vibrationally excited bending states of N_2O have much larger Franck-Condon overlap with the dissociative state than does the (000) mode. This is corroborated by the large observed temperature dependence of the N_2O cross section [*Merienne, et al.*, 1990, and refs therein]. By deconvolving the cross section data at 225 and 296 K [*Selwyn et al.*, 1977] into contributions from the (000) and (010) modes, we calculate that the 213 nm cross section of N_2O (010) is approximately 15 times larger than that of N_2O (000). This implies that, although only 10% of the N_2O molecules are in the first excited bending mode (010) at 298 K, more than 50% of the photolysis at 213 nm occurs via the

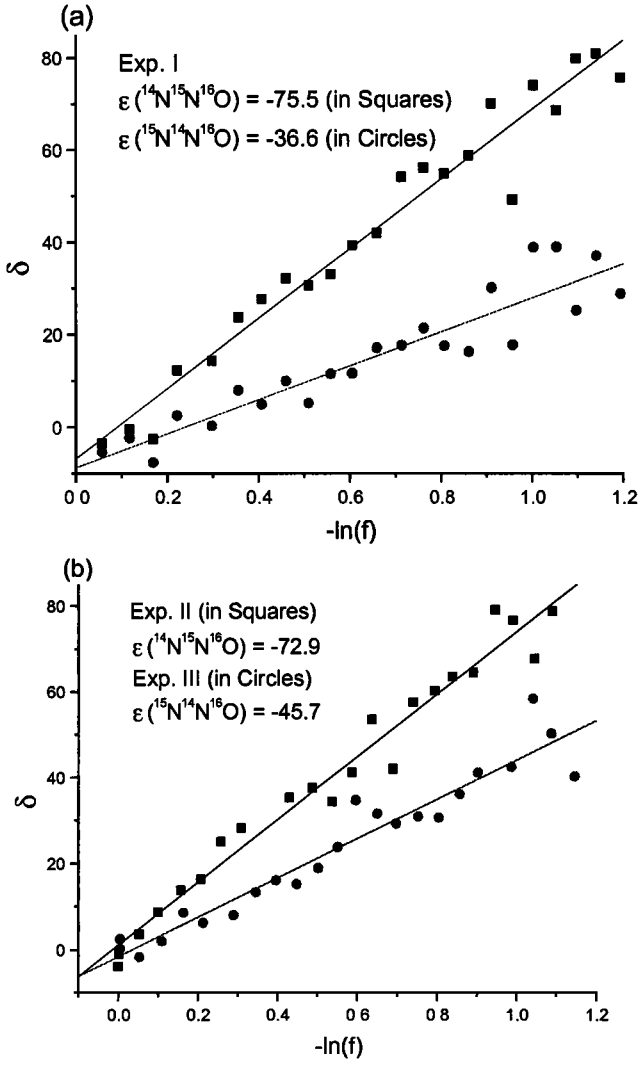

Figure 3. The fractionation data from 213 nm photolysis, fitted to a Rayleigh fractionation model. $\delta = (R_i / R_{std} - 1) \times 1000$, where the R's are the slow-to-fast photolysis isotopic ratio. R_{std} is for the pre-photolysis samples and R_i is for the photolyzed samples. f is the fraction of N_2O remaining. $\epsilon(^{15}N^{14}N^{16}O) = \epsilon(^{15}N^{14}N^{16}O$ / $^{14}N^{14}N^{16}O)$ and $\epsilon(^{14}N^{15}N^{16}O) = \epsilon(^{14}N^{15}N^{16}O$ / $^{14}N^{14}N^{16}O)$. (a) In Experiment I, three N_2O isotopomers are photolyzed; (b) In Experiment II, a mixture of $^{14}N^{15}N^{16}O$ and $^{14}N^{14}N^{16}O$ is photolyzed; while in Experiment III, a mixture of $^{15}N^{14}N^{16}O$ and $^{14}N^{14}N^{16}O$ is photolyzed.

excited vibrational states. The changes in the potential energy surface for various N_2O isotopomers are different for the two vibrational modes, which leads to different wavelength shifts of the cross sections according to YM97. Therefore, including the vibrationally "hot" molecules in the fractionation calculation is necessary for a quantitative comparison to the experimental results.

The preceding argument implicitly assumes that the photodissociation of N_2O occurs via the repulsive $B(^1\Delta)$ electronic state, as YM97 did in light of the available data at that time. As *Neyer et al.* [1999] have demonstrated, however, the dynamics of this photodissociation are more complex than previously thought, with more than one electronic state involved in the excitation / dissociation. It is possible that the two different ground state vibrational modes may have distinct coupling with the upper states, which will further complicate the spectroscopy.

The large differences in the UV cross sections of the various N_2O isotopomers observed in this study support YM97's suggestion that this mechanism is responsible for the isotopic fractionation observed in the stratosphere. A fully quantitative test of this theory, however, requires accurate wavelength and temperature dependent differential cross sections for these compounds; the use of simple theoretical models for prediction of these cross sections has been ruled out by this study and the previous work of *Rahn et al.* [1998]. The difference in the cross sections of the isotopomers examined here is large enough that a classical Beer's law study of the isotopomers (which are available commercially in high purity) can provide the required spectroscopic data.

Acknowledgments. We would like to thank the NSF MRI program for the photolysis laser, CASIX Inc. for the BBO crystals and the Dreyfus Foundation for the FTIR spectrometer used in this study. Vincent Wu acknowledges financial support from an anonymous donor through a Caltech Summer Undergraduate Research Fellowship.

References

Cliff, S. S., and M. H. Thiemens, The $^{18}O/^{16}O$ and $^{17}O/^{16}O$ ratios in atmospheric nitrous oxide: A mass-independent anomaly, *Science, 278,* 1774-1776, 1997.

DeMore, W. B., S. P. Sander, D. M. Golden, R. F. Hampson, M. J. Kurylo, C. J. Howard, A. R. Ravishankara, C. E. Kolb, and M. J. Molina, *Chemical kinetics and photochemical data for use in stratospheric modeling, JPL Publication 97-4,* NASA/JPL, Pasadena, California, 1997.

Fritz, P., and J. Ch. Fontes (Eds.), *Handbook of environmental isotope geochemistry, volume 1, the terrestrial environment, A,* 545 pp., Elsevier, New York, 1980.

Houghton, J. T., L. G. Meira Filho, J. Bruce, H. Lee, B. A. Callander, E. Haites, N. Harris and K. Maskell (Eds.), *Intergovernmental panel on climate change, climate change 1994: radiative forcing of climate change and an evaluation of the IPCC IS92 emission scenarios,* Cambridge University Press, New York, 1995.

Kim, K.-R., and H. Craig, Two isotope characterization of N_2O in the Pacific Ocean and constraints on its origin in deep water, *Nature, 347,* 58-61, 1990.

Kim, K.-R., and H. Craig, Nitrogen-15 and oxygen-18 characteristics of nitrous oxide: A global perspective, *Science, 262,* 1855-1857, 1993.

Merienne, M. F., B. Coquart, and A. Jenouvrier, Temperature effect on the ultraviolet absorption of $CFCl_3$, CF_2Cl_2 and N_2O, *Planet. Space Sci., 38,* 617-625, 1990.

Naqvi, S. W. A., T. Yoshinari, D. A. Jayakumar, M. A. Altabet, P. V. Narvekar, A. H. Devol, J. A. Brandes, and L. A. Codispoti, Budgetary and biogeochemical implications of N_2O isotope signatures in the Arabian Sea, *Nature, 394,* 462-464, 1998.

Neyer, D. W., A. J. R. Heck, and D. W. Chandler, Photodissociation of N_2O: J-dependent anisotropy revealed in N_2 photofragment images, *J. Chem. Phys., 110,* 3411-3417, 1999.

Rahn, T., and M. Wahlen, Stable isotope enrichment in stratospheric nitrous oxide, *Science, 278,* 1776-1778, 1997.

Rahn, T., H. Zhang, M. Wahlen, and G. A. Blake, Stable isotope fractionation during ultraviolet photolysis of N_2O, *Geophys. Res. Lett., 25,* 4489-4492, 1998.

Selwyn, G., J. Podolske, and H. S. Johnston, Nitrous oxide ultraviolet absorption spectrum at stratospheric temperatures, *Geophys. Res. Lett., 4,* 427-430, 1977.

Wahlen, M., and T. Yoshinari, Oxygen isotope ratios in N_2O from different environments, *Nature, 313,* 780-782, 1985.

World Meteorological Organization, *Scientific assessment of ozone depletion: 1994, global ozone research and monitoring project-report 37,* World Meteorological Organization, Geneva, Switzerland, 1995.

Yoshida, N., N-15-depleted N_2O as a product of nitrification, *Nature, 335,* 528-529, 1988.

Yoshinari, T., and M. Wahlen, Oxygen isotope ratios in N_2O from nitrification at a wastewater treatment facility, *Nature, 317,* 349-350, 1985.

Yoshinari, T., *et al.*, Nitrogen and oxygen isotopic composition of N_2O from suboxic waters of the eastern tropical north pacific and the arabian sea - measurement by continuous-flow isotope-ratio monitoring, *Marine Chem., 56,* 253-264, 1997.

Yung, Y. L., and C. E. Miller, Isotopic fractionation of stratospheric nitrous oxide, *Science, 278,* 1778-1780, 1997.

H. Zhang, P. O. Wennberg, and G. A. Blake, Division of Geological and Planetary Sciences, M/S 150-21, California Institute of Technology, Pasadena, California 91125. (e-mail: hui@gps.caltech.edu; wennberg@gps.caltech.edu; gab@gps.caltech.edu)

V. H. Wu, St. Catharine's College, University of Cambridge, Cambridge, CB2 1RL, UK. (e-mail: vw205@hermes.cam.ac.uk)

(Received November 14, 1999; accepted February 29, 2000.)